The University of Maine
DigitalCommons@UMaine

Electronic Theses and Dissertations | Fogler Library

Fall 12-15-2023

Elucidating the Pd Active Sites of Bimetallic Gold-palladium Catalysts Using Chemisorption and Titration Techniques

Andrew T. Boucher
University of Maine, andrew.boucher@maine.edu

Follow this and additional works at: https://digitalcommons.library.umaine.edu/etd

 Part of the Physical Chemistry Commons

Recommended Citation

Boucher, Andrew T., "Elucidating the Pd Active Sites of Bimetallic Gold-palladium Catalysts Using Chemisorption and Titration Techniques" (2023). *Electronic Theses and Dissertations*. 3907.
https://digitalcommons.library.umaine.edu/etd/3907

This Open-Access Thesis is brought to you for free and open access by DigitalCommons@UMaine. It has been accepted for inclusion in Electronic Theses and Dissertations by an authorized administrator of DigitalCommons@UMaine. For more information, please contact um.library.technical.services@maine.edu.

ELUCIDATING THE PD ACTIVE SITES OF BIMETALLIC GOLD-PALLADIUM CATALYSTS USING CHEMISORPTION AND TITRATION TECHNIQUES

By

Andrew Thurstan Boucher

Bachelor of Science in Chemistry Saint Michael's College, 2018

A THESIS

Submitted in Partial Fulfillment of the

Requirements for the Degree of

Master of Science

(in Chemistry)

The Graduate School

The University of Maine

December 2023

Advisory Committee

Brian G. Frederick, Associate Professor of Chemistry, Co-Advisor

Thomas J. Schwartz, Associate Professor of Chemical Engineering, Co-Advisor

François G. Amar, Professor of Chemistry, Committee member

© 2023 Andrew Thurstan Boucher

All Rights Reserved

ELUCIDATING THE PD ACTIVE SITES OF BIMETALLIC GOLD-PALLADIUM CATALYSTS USING CHEMISORPTION AND TITRATION TECHNIQUES

Andrew Thurstan Boucher

Thesis Co-Advisors: Dr. Brian G. Frederick and Dr. Thomas J. Schwartz

An Abstract of the Thesis Presented
In Partial Fulfilment of the Requirements for the
Degree of Master of Science in Chemistry
December 2023

A bimetallic nanoparticle catalyst combines two different metals on an oxide support, which can increase the selectivity towards useful products that may be too tightly bound to a monometallic catalyst. To explore the surface properties of such a system, we made a group of four PdAu bimetallic catalysts with varying gold mass loadings to compare with a parent Pd catalyst. The parent catalyst was synthesized using ion exchange, and gold was added to this parent Pd catalyst using incipient wetness impregnation (IWI) to create four bimetallic catalysts. All catalysts were characterized using H_2 and CO chemisorption in tandem with O_2 and H_2 titration methods. The measured dispersion of the parent catalyst ranged from 60-72% which is consistent with previous measurements for catalysts synthesized with the same loading and synthesis technique. This dispersion value implies an average Pd particle diameter of about 1.8 nm. Each bimetallic catalyst was characterized using chemisorption and titration methods and the fractional gold coverage was found to be about 70%, independent of the gold loading. In parallel with the chemisorption and titration measurements, we used ICP-OES analysis to determine the gold content in the bimetallic catalysts, but these results were inconsistent with the quantities of gold used in the IWI synthesis.

ACKNOWLEDGEMENTS

I would first like to express my deepest love and gratitude to my life partner Nancy Khattar. Without her patience and devotion in times of hardship, I would not be where I am at today. She reminds me to persevere no matter what obstacles and challenges come my way. I would also love to thank her family and mine for always giving me comforting hospitality where I could recollect my thoughts and strengthen relationships with every member. I also want to thank my many friends and colleges for helping in long assignments and practice presentations, and for many well needed weekend trips and celebrations.

I want to thank all members and friends in my UMaine catalysis research group. While my research journey has not always been a smooth path, everyone has helped forge me into the scientist I am today. Thank you to the many seminar practice presentations, long discussions of research ideas and results, and many fun adventures outside of research. Thank you both Dr. Brian Frederick and Dr. Thomas Schwartz who have taught me to be a much more careful thinker in slowing down how I can express my own scientific thoughts, how to be a more methodical experimentalist in organizing the steps and reasons behind specific techniques, and how to qualitatively understand results at fundamental levels. The level of patience and understanding you have given is truly valued.

I would like to also thank Suzanne Perron for her in acquiring ICP-OES data.

TABLE OF CONTENTS

LIST OF TABLES

LIST OF FIGURES

CHAPTER 1- INTRODUCTION

1.1 What is a bimetallic catalyst?

The basic principle of a catalyst is to make a chemical process that produces specific compounds more efficient and energetically favorable. For example, one way a catalyst is useful is to remove methane (a known greenhouse gas) from the exhaust of natural gas engines.[1] Palladium based catalysts, both monometallic and bimetallic, have been widely studied in this methane removal mechanism, specifically in the process of methane oxidation. Recent studies of Pd and Pd-Pt have shown that the bimetallic Pd-Pt catalysts has better long-term stability, catalytic activity, and higher sulfur tolerance than supported Pd monometallic catalysts.[2]

There are several definitions for what a bimetallic catalyst is, especially with regards to the distinction between surface and bulk alloys. Ponec et al. inquire what is meant by alloying and how this consideration applies to bimetallic catalysts.[3] An alloy is a metallic system that contains two or more components regardless of how they are mixed. In the case of bimetallic catalysts of interest, they are specifically "surface alloys". For example, in a Pd-Au/SiO_2 bimetallic catalyst with an average particle size of 1 nm, the Au and Pd atoms are supported on silica gel. The silica is used as a carrier for the PdAu clusters. These differ from bulk alloys because nearly every metal atom in the small, supported cluster is exposed to the surface.[4] In contrast, at low dispersion (e.g., <20%), a significant fraction of metal atoms are not on the surface of the nanoparticle and instead embedded within the cluster, and they may behave closer to bulk materials.

In bimetallic systems with high metal dispersion, one can consider a spectrum of inter-metallic interactions depending on segregation, mixing, or other morphologies.[5] The catalytic performance can depend the system morphology, based on conditions including metal type,

support type, size of nanoparticles, temperature and pressure of the reaction, and even reduction and calcination conditions. Sinfelt studied some of these possibilities in earlier work in a hydrogenolysis reaction of ethane to methane using various bimetallic combinations of group VIII and group IB metals. He learned that the activity of group VIII metals was many orders of magnitude greater than that of group IB metals and that using the combination of the two metal types improved the activity by three orders of magnitude compared to monometallic group VIII supported metal catalyst.

1.2 Applications of bimetallic catalysts

The idea that combining two metals on a support can improve the performance of the bimetallic catalyst compared to a monometallic catalyst has been applied in many catalytic reactions to improve selectivity, activity, and conversion. In another example, the performance of both monometallic and bimetallic catalysts was compared in an aqueous phase reforming (APR) study.[6] Biomass derivatives were combined with the catalysts in aqueous solution at controlled temperatures and pressures to produce hydrogen and other products. The APR process involves both C-C bond cleavage of oxygenates such as ethylene glycol and water-gas-shift (WGS) that converts CO and H_2O to CO_2 and H_2. Using platinum as a parent catalyst and a second metal like Ni, Co, or Fe improved the catalytic activity during the WGS pathway thereby increasing carbon dioxide and hydrogen production rates. The conversion of ethylene glycol using Pt/Al_2O_3 compared to the conversion using $1.15Pt/0.35Ni/Al_2O_3$ was improved from 1.4% to 79%.[7] Such significant improvement can be explained using Density Functional Theory (DFT). According to DFT studies, a catalyst that contains both platinum and nickel causes a decrease in the d-band density of states compared to a catalyst with only platinum.[34] It has been shown that this shift to

a lower d-band correlates to a decrease in CO binding energy and further facilitates the WGS pathway.

In a second example comparing bimetallic and monometallic catalysts, the hydrogenolysis reaction of ethane was studied by Sinfelt et al.[8] In this specific example, the activity of the reaction was measured at varying atomic copper compositions while keeping the atomic composition of ruthenium constant in a Cu-Ru/Al_2O_3 catalyst. They discovered that when copper and ruthenium have a 1:1 atomic composition ratio the activity is reduced by three orders of magnitude relative to the same reaction using a pure Ru/Al_2O_3 catalyst. In this case, the addition of a second metal type causes a decrease in activity during the hydrogenolysis reaction.

For a Pd-Au bimetallic catalyst, gold atoms are believed to be less active compared to palladium atoms during catalytic reactions; therefore, gold acts as an inert metal relative to palladium.[9] The influence of impacting the selectivity for the reduction of furfural in water was studied by Modelka et al. using Pd-Au/SiO_2 bimetallic catalysts.[11] The catalysts were prepared via co-impregnation on silica with aqueous solutions of $PdCl_2$ and $AuCl_3$ containing 5 wt % palladium and 0.5, 1, 2, 5, and 10 wt % Au. By using catalysts containing a higher amount of gold while keeping the palladium loading constant, one would expect less available active sties on the catalyst surface. This directly impacts product selectivity in the reaction.

It was found that using these Pd-Au/SiO_2 bimetallic catalysts for reduction of furfural resulted in a large range of possible products like furfuryl alcohol, tetrahydrofurfuryl alcohol, 5-hydroxy-2-pentanone, and 2-methyloxolan-2-ol.[11] By using catalysts with increasing gold weight percent, the selectivity towards furfuryl alcohol and 5-hydroxy-2-pentanone decreased and the selectivity towards tetrahydrofurfuryl alcohol increased. The authors also discovered that crystal size of Au and dispersion of Pd impacted the product distribution. Through XRD evidence of

determining crystal size according to the Scherrer equation, it was found that crystal size of palladium clusters did not change significantly (5.4 nm-7.8 nm) upon adding more wt % Au but the crystal size of Au clusters did change significantly (8.4 nm -43.4 nm). The formation of 2-methyloxolan-2-ol was favored at a small Au crystal size of 8.4 nm (1 wt% Au) and formation of tetrahydrofurfuryl alcohol was favored at a larger crystal size of 41.3 nm (5 wt% Au).

1.3 Geometric and electronic effects

A "geometric effect" occurs when a less active metal dilutes the atoms of a more active metal thus decreasing the size of homogenous regions on the catalytic surface.[10] Alloying two metals in this way on an oxide carrier can cause a lattice mismatch from the atom displacement which in turn can cause changes in the d-band location thus impacting the activity of the catalyst. One type of geometric effect is described by Nørskov et al. as a strain effect in which there is surface alloy within the lattice consisting of two metals.[13]A metal of one phase is not simply grown on another metal in a different phase but rather there is a local deformation of one metal phase caused by the other metal.

This strain effect can be utilized to impact the chemisorption properties of the catalyst. Nørskov et al. computationally studied a metal Ru(0001) slab under both tensile and compressive stress in order to show that the chemisorption energies as well as barriers are different on strained lattices. This can be applied to several catalytic systems. They implemented a surface strain by changing the equilibrium lattice constant parallel to the surface between 2.7-2.8 Å for CO and O chemisorption and found that bond strength of both increases the greater the lattice constant. The trend found by Nørskov follows experimental STM oxygen adsorption studies on Ru(001) strained surfaces because oxygen was found to adsorb on sites at the outer

region of the surface.[25] This would correspond to a high binding energy at a large equilibrium lattice constant distance. Results of CO adsorption were hard to interpret because CO was very mobile on the surface. This resulted in small differences in binding energies between different types of adsorption sites.

Another aspect to consider is how the charge distribution of sites can impact what chemistry can occur on the surface. This falls under "electronic effects" where the local electronic properties of one metal atom type are impacted by the electronic properties of another atom. Going back to the APR example discussed earlier, there was a decrease in the d-band strength by alloying two metals causing a decrease in binding energy of CO and H_2.[5] This allowed more active sites to be available for the reaction.

The development of the d-band model of catalysis came following several theories that had previously attempted to explain the effect of bimetallic catalysts. According to Rigid Band Theory, for a metal to have catalytic activity, it must have a high density of states at the Fermi level and an incomplete electron filled d-band orbital.[14] Furthermore, metal A and metal B have the same electronic structure and a change in catalytic activity results in changing the entire alloy rather than individual metal A or metal B. This theory does not consider the composition of an alloy at the surface.

The next level of theory was established by Jacobsen and was referred to as the Effective Medium Theory, where the composition of an alloy at the surface did matter.[15] This theory describes density-dependent energy of overlapping atoms in a condensed system where the total energy of any metal atom in a system is impacted by the effects of other surrounding atoms. The currently established theory now used is the d-band model which expands on the effective medium theory. This model, which is described in a study by Nørskov et al., shows molecular

and atomic binding energy as a function of d-band centers (the center of the d-type density of states in an atomic sphere that is centered at an atom on the surface) for various transition metal surfaces.[13] They show that adsorbates interact with the same metal atoms in the same local geometry; however, changing the number of neighboring metal atoms changes the adsorption energy, as seen in Figure 4 of that study. The difference in the distances changes the d-band center because of the change in electron density of the metal atoms.

This distance can be changed by adding another metal in a surface alloy such as in the case of a bimetallic catalyst, and this can impact how favorably an adsorbate binds to a surface. For example, a study by Ruban and Nørskov investigates whether CO binds more strongly on a bimetallic Cu/Pt(111) surface vs a single monolayer Cu(111) surface.[16] This trend also holds for the case for Ni(111) and Ni/Ru(0001). What Ruban and Nørskov conclude is that CO chemisorption energy depends on the shift in d-band centers. After normalizing the shift in CO adsorption energy predicted with their model and plotting this against shifts in d-band centers in Figure 2[16] from the study, a trend can be seen where a shift in d-band center towards higher energy corresponds to a greater adsorption energy of CO.

In Table 1 of the same study[16], the evidence indicates an upshift in d-band centers when a small radius metal element is alloyed with a larger metal. This corresponds to an increase in CO binding energy. Alternatively, when a large metal is alloyed with a smaller metal surface there is a shift towards lower d-band centers and an expected decrease in CO binding energy. For example, when nickel is alloyed on a palladium surface compared to gold alloyed on a pallidum surface, there is a downshift in d-band center from 0.54 eV to -0.14 eV suggesting that CO binds more favorably on a Ni/Pd surface compared to a Au/Pd surface.

1.4 Characterization techniques

What has been described so far includes definitions of bimetallic catalysts, ways in which they are applied, and geometric and electronic properties that are of interest. Next, characterization techniques will be discussed. Using characterization techniques, specific aspects of bimetallic catalysts can be learned, including volumetric uptakes on metallic active sites, metal dispersion on the oxide carrier, and particle size based on dispersion. Furthermore, by using these techniques one can make comparisons of various bimetallic systems.

In XRD characterization work by Bonarowska et al., they studied both palladium and pallidum-gold catalysts.[17] The monometallic catalyst was synthesized in two different ways, one being ion-exchange and the other being incipient wetness impregnation. If palladium were highly dispersed on the surface, one would expect to observe a broad peak in the X-ray diffractogram for the (111) plane compared to if there were large clusters of palladium atoms. In the diffractogram, they observed a narrow peak in the catalyst made via wetness impregnation compared to the catalyst made via ion excahnge. One advantage of using XRD in this case is that particle sizes can be studied (if the particles are larger than ~2 nm) in looking at two different experimental ways to synthesize a monometallic catalyst.

Expanding more on XRD in this study, Bonarowska et al. also evaluated the XRD patterns of Pd-Au/SiO_2 bimetallic catalysts and specifically looked at variations in structure and phase compositions under reduction conditions. They found for a catalyst with 80 mol % palladium and 20 mol % gold that there was a noticeable change in the X-ray diffractogram before and after reduction in hydrogen at 400˚C. After the deposition reaction to make the bimetallic catalyst, it was observed that two separate fractions of highly dispersed monometallic gold and monometallic palladium atoms existed on the surface at the same time. After only a

one-hour reduction, the gold phase was no longer observed, a new Pd-Au combination peak was formed, and a smaller amount of pure palladium was observed. This could indicate that all the gold alloyed with the palladium leaving some monometallic palladium sites exposed if the nanoparticle size was greater than 2 nm. Below this particle size limit, XRD peaks are too broad, and it would be impossible to tell from XRD evidence how the surface composition is affected by reducing for various time periods.

In the application of chemisorption and titration techniques to Pd-Au/SiO_2 bimetallic catalysts, the Pd surface site density can be determined because metal surface atoms can be probed and counted at the molecular level by selective adsorbate gasses.[18] CO chemisorption occurs non-dissociatively and can be a useful probe molecule for palladium characterization. CO can bind to metal sites in a stoichiometry of 1:1 (linear) or 1:2 (bridged) as seen in the schemes below:

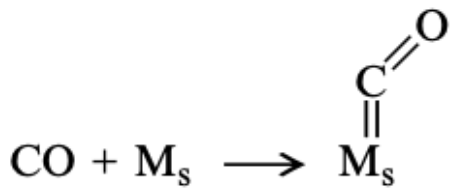

[Linear- 1:1 CO/M]

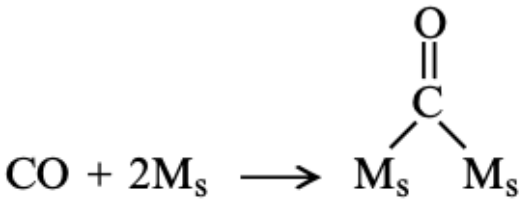

[Bridged- 1:2 CO/M]

Early on, it was suggested based on evidence of H_2, O_2 and CO chemisorption that the best approximation for CO adsorption to most metal sites, including palladium, is to assume a

1:1 ratio.[19] As the weight percent of gold loading increases, more palladium atoms share an oxidation state with Au, and less pure palladium sites are available for CO adsorption.

Another sensitive gas adsorption technique is a hydrogen-oxygen titration reaction where either a pre-existing monolayer of oxygen is titrated with H_2 or a pre-existing monolayer of hydrogen is titrated with O_2, first proposed by Benson and Boudart as shown below:[22]

Hydrogen Titration: $Pd_SO + \frac{3}{2} H_2 \rightarrow Pd_SH + H_2O$ (1.1)

Oxygen Titration: $Pd_SH + \frac{3}{4} O_2 \rightarrow Pd_SO + \frac{1}{2} H_2O$ (1.2)

In accordance with equation 1.1, the palladium on the surface can be passivated by oxygen atoms at 298 K. This creates a thin layer of oxygen on the Pd (which is still metallic) that can then be titrated with hydrogen gas. During this titration process, the silica support should adsorb the water in the reaction; therefore, one can quantify the amount of gas phase hydrogen adsorption using volumetric dosing. This technique also has a higher sensitivity over CO chemisorption because of an increased stoichiometry of adsorbate per palladium atom (from 1 CO/Pd to 1.5 H_2/Pd).

An important parameter that can be quantified using these chemisorption and titration techniques that is able to differentiate bimetallic catalysts by surface composition is the dispersion of metal atoms on a support. Vannice defines dispersion as the ratio of the number of metal atoms on the surface of the nanoparticle to the total number of metal atoms in the nanoparticle and this expression can be seen in equation 1.3.[18]

$$Metal\ Dispersion\ = \frac{mols\ of\ surface\ metal}{mols\ of\ total\ metal} \quad (1.3)$$

Another factor that must be considered during chemisorption measurements is Pd hydride formation. This effect has been studied most recently by Sibel et al. during gas phase reactions using XAFs and EXAFS.[21] They address what a palladium hydride phase is, why does it matter for a reaction, how can it be understood and quantified, and what conditions are required to avoid it if desired. More recent studies involve calibrating changes in quick scanning X-ray absorption spectroscopy (QEXAFS) spectra with temperature-programmed reduction to quantitatively evaluate Pd hydride formation.[32] Benson and Boudart discuss practical conditions for carrying out hydrogen titration and mention that palladium hydride formation can be avoided by keeping the hydrogen pressure below 2.27 kPa at 303K or below 46.7 kPa at 373K, and evacuation at room temperature.[22] If one is doing hydrogen titration of chemisorption to quantify palladium dispersion, steps must be taken to break beta-hydride that is formed during reduction.

1.5 Synthesis techniques of supported Pd-Au nanoparticles

One synthesis technique to make catalysts like a 2 wt% Pd/SiO_2 is incipient wetness impregnation (IWI) where an aqueous solution of palladium dichloride is added to a silica slurry.[17] The slurry is well mixed, and capilary action draws the palladium into the pore structure, where it binds to the support. A very interesting point made by Bonarowska et al. is a qualitative example of why their use of incipient wetness impregnation did not result in a consistent particle size distribution in a Pd/SiO_2 catalyst. Upon visual inspection it was found that the catalyst made with this technique did not have a consistent grey color but rather contained black and very dark grains, thus indicating that very large Pd nanoparticles were present. This was confirmed in their XRD results where the particle size was determined to be 100 nm, suggesting these Pd particles exist outside of the silica pore structure. In the same study,

they synthesized another 2 wt% Pd/SiO_2 catalyst by the technique of ion exhange using an aqueous solution of $Pd(NO_3)_2 \cdot 4NH_3$ and a silica slurry under a basic pH. In this method, there is a reversible interchange of one ion that is contained in a solid with a like-charge ion present in a solution surrounding the solid. This technique resulted in much more homogenous crystal clusters of smaller size between 10-15 nm. A bimetallic Pd-Au/ SiO_2 can also be made using incipient wetness impregnation by adding an aqueous solution of a gold salt like $HAuCl_4$ to Pd/SiO_2.

Another way to make a catalyst with two metals is to make a colloidal metal suspension of Au and Pd particles suspended in an alcohol in the presence of polyvinylpyrrolidone (PVP).[24] The advantage of using PVP is that it prevents the suspended particles from agglomerating, and this results in a more favorable and more monodispersed particle size distribution than something like incipient wetness impregnation. This technique has produced Pd-Au catalysts that have outperformed either monometallic Pd or Au catalysts such as in the work of Pawelec et al. with aromatic hydrogenation.[25] The activity of naphaline production normalized to palladium loading, for example, was highest using the Au-Pd/SiO_2 catalyst prepared using PVP compared to the same catalyst synthesized using wetness impregnation. However, using a high calcination temperature of 400˚C to remove the organic binder can change the catalyst structure in such a way that the optimum composition may not be achieved.[12]

Once a parent catalyst is made with one metal on the support, the technique of electroless deposition can be utilized where a 2nd metal is catalytically deposited only on the pre-existing metal and not the support such as shown in the reaction scheme below:[23]

$$\mathbf{N} + \mathbf{M}^{z+}(\mathbf{aq}) + \mathbf{RA}(\mathbf{aq}) \rightarrow \mathbf{M{-}N} + \mathbf{Ox}(\mathbf{aq}) \quad (1.4)$$

In the above redox reaction, an aqueous reducible salt (M^{z+}) is reduced by the reducing agent (RA) to deposit the secondary metal on the catalytic nuclei (N) to form a bimetallic catalyst in a stoichiometric reaction producing the oxidized form of the RA. Furthermore, the difference in electrochemical potential between gold and palladium is what allows Au to be deposited over a "less-noble" Pd metal. The reaction can also continue auto-catalytically where multiple layers of M can occur to form multiple shells. Because the reduction of the Au takes place catalytically in solution using hydrazine as a reducing agent, these mild reduction conditions (*e.g.*, compared the high-temperature reduction needed following IWI) leads to negligible effects of changing the ensemble configuration due to temperature.

CHAPTER 2- EXPERIMENTAL

2.1 Synthesis

1) Ion Exchange

To make the Au-Pd/SiO_2 bimetallic catalysts, a 2 wt% Pd/SiO_2 parent catalyst was first prepared by ion exchange of $Pd(NO_3)_2{\cdot}4NH_3$ (Sigma Aldrich 10 wt% $Pd(NO_3)_2{\cdot}4NH_3$ solution in water) on silica gel following the procedure described by Schwartz et. al.[28] The silica gel was first crushed and sieved between 50 and 100 mesh. 5.0014 grams of SiO_2 silica gel was suspended in 125 mL of Milli-Q water and then concentrated NH_4OH (10 wt%) was added to raise the pH to 11. Finally, 2.864 grams of the aqueous $Pd(NO_3)_2{\cdot}4NH_3$ (10 wt%) solution was added and the mixture was magnetically stirred for 1 hour. The catalyst was dried in air at 383 K for 3 hr, calcined in flowing air at 573 K, reduced in flowing hydrogen at 533 K, and passivated in oxygen. It should be noted that 0.2864 grams of $Pd(NO_3)_2{\cdot}4NH_3$ corresponds to 0.1024 grams of palladium and this results in a palladium loading of 192 μmol Pd/ g catalyst. This loading will be important for the discussion later.

2) Wetness Impregnation

Four Pd-Au/SiO_2 catalysts were made using a measured mass of chloroauric acid hydrate (seen in the Table 2.1) dissolved in Milli-Q water for each intended gold loading sample. The incipient wetness impregnation point for approximately 0.7 grams of the parent catalyst was found to be about 1.34 grams of Milli-Q water. Each $HAuCl_4$ sample was then dissolved in that measured amount of water and this solution was added to approximately 0.7 grams of the parent catalyst and mixed. The chloroauric acid hydrate was freshly prepared from Sigma Aldrich and is hygroscopic meaning the actual mass of gold loading may be less than the value massed out on

scale due to absorption of atmospheric water. The bimetallic catalyst samples were dried at 90˚C overnight and next reduced by heating at a 2˚C/min ramp rate in flowing hydrogen and holding at 260˚C for 2 hours.

3) Aqua Regia Digestion

Gold compositions were confirmed with ICP. To prepare the catalyst samples for this analysis, as described by Schwartz et al., approximately 50 mg of each catalyst sample was digested in 5 mL aqua regia for 4 hours at 140˚C under magnetic stirring.[28] Each batch of aqua regia was made by adding approximately 1.25 grams of nitric acid to 3.75 grams of hydrochloric acid. The actual experimental masses can be seen in Table 1. After digestion, each sample batch was diluted with about 50 grams of DI water to be above a 10 ppm ICP detection limit and after this step, the samples were ready for ICP analysis. Analysis was performed at UMaine by the Soil Science Laboratory, using gold calibration standards.

Table 2.1: Experimental masses for each bimetallic Pd-Au/SiO_2 sample during a) wetness impregnation and b) aqua-regia digestion and dilution.

Sample	$HAuCl_4 \cdot nH_2O$(g)[a]	Pd/SiO_2(g)[a]	Water(g)[b]	Aqua-regia (g)[b]	Pd-Au/SiO_2 (g)[b]
AuPd-1	0.00924	0.7008	58.000	5.006	0.052
AuPd-2	0.0121	0.7009	50.994	5.044	0.066
AuPd-3	0.0194	0.7006	52.942	5.165	0.050
AuPd-4	0.02515	0.6997	58.910	5.149	0.054

2.2 Characterization

A Micromeritics ASAP 2020 instrument was used for chemisorption of H_2 and CO and titration of H_2 and O_2. Special care was taken to avoid the formation of beta palladium hydride phase as described by Benson and Boudart by performing hydrogen analysis at either 35˚C and below 17 torr or at 100˚C and below 350 torr.[22] Three sets of experiments were performed on all catalysts as described below, and for each set a leak test was performed by the software and all reported results have a leak rate less than 10 μtorr/min.

1) First set:

The catalysts were pretreated by being reduced in H_2 at 350˚C, cooled to 35˚C and evacuated, and then analyzed using hydrogen chemisorption. It was expected that chemisorbed

hydrogen uptake should decrease with increasing gold. Once this trend was verified, all four gas adsorption measurement techniques were performed on approximately 100 mg of the parent catalyst and then on the 4 Pd-Au bimetallic catalysts in this order for the second set.

2) Second set:

1) One hour reduction in flowing hydrogen at 350˚C followed by a one hour evacuation after cooling the sample to 35˚C and then hydrogen chemisorption was done at 35˚C, 2) oxygen titration of the hydrogen remaining from step 1 at 35˚C, 3) hydrogen titration of the oxygen remaining from step 2 at 100˚C followed with an evacuation at 100˚C to desorb any remaining hydrogen, and 4) CO chemisorption at 35˚C.

3) Third set:

To show reproducibility, all four techniques were repeated in the same sequence for the AuPd-3 catalyst. Also, an independent H_2 titration set of experiments were conducted on 3 of the bimetallic catalysts (AuPd-2,-3,and -4) to verify the linear response in uptake using titration and whether there were any differences between a technique used in tandem and a technique used independently. This followed the method described by Boudart et al. The catalysts were reduced at 350˚C, evacuated, and then cooled to 100˚C, pretreated with flowing oxygen at 100˚C for one hour, evacuated at the same temperature for 1 hour, and then analyzed at 100˚C via hydrogen titration.

CHAPTER 3- RESULTS AND DISCUSSION

3.1 Monometallic 2 wt % Pd/SiO_2 parent catalyst

The dispersion of the parent 2 wt% Pd/SiO_2 catalyst was characterized using chemisorption methods. The isotherm chemisorption profiles on the parent catalyst shown in Figure 3.1 are consistent with expected results as described by Vannice.[31] The isotherm with the greatest uptake corresponds to adsorption on the palladium plus the support. The catalyst is then evacuated at the analysis temperature and a second isotherm is measured. The isotherm with the smaller uptake is adsorption only on the support, because the adsorbates that are already bound to palladium sites are not desorbed during evacuation but those on the support are physisorbed and desorb. Therefore, the difference between the two isotherms is the amount of adsorbate bound on palladium. Furthermore, following the logic described by Vannice, chemisorption of either CO or H_2 on an unsupported Pd surface can be represented by a Langmuir type isotherm of adsorbate uptake vs. adsorbate pressure. For example, the adsorption of H_2 on the pure silica support is a weak and reversible interaction that is usually described by Henry's Law and represented in the isotherm with the lowest uptake seen in Figure 3.1A. The interaction of H_2 on pure palladium is much stronger where a chemical bond is formed with a binding energy of about 1eV. The isotherm with the largest uptake represents the contributions of both a weak interaction and a strong chemisorption influence. Therefore, the difference between these two isotherms represents the binding of only hydrogen to palladium and can be used to count the number of exposed palladium atoms.

The difference between the uptake in the 1st and 2nd isotherms, shown in Table 3.1, is 56 ±1 μmol H_2/g. The palladium site density takes into account the stoichiometry of the reaction

$$H_2 + 2Pd \rightarrow 2PdH, \tag{3.1}$$

and therefore, the palladium site density is 112 ± 2 µmol/g. The dispersion can be calculated directly from the ratio of the Pd site density to the Pd loading of 192 µmol/g to be 58%.

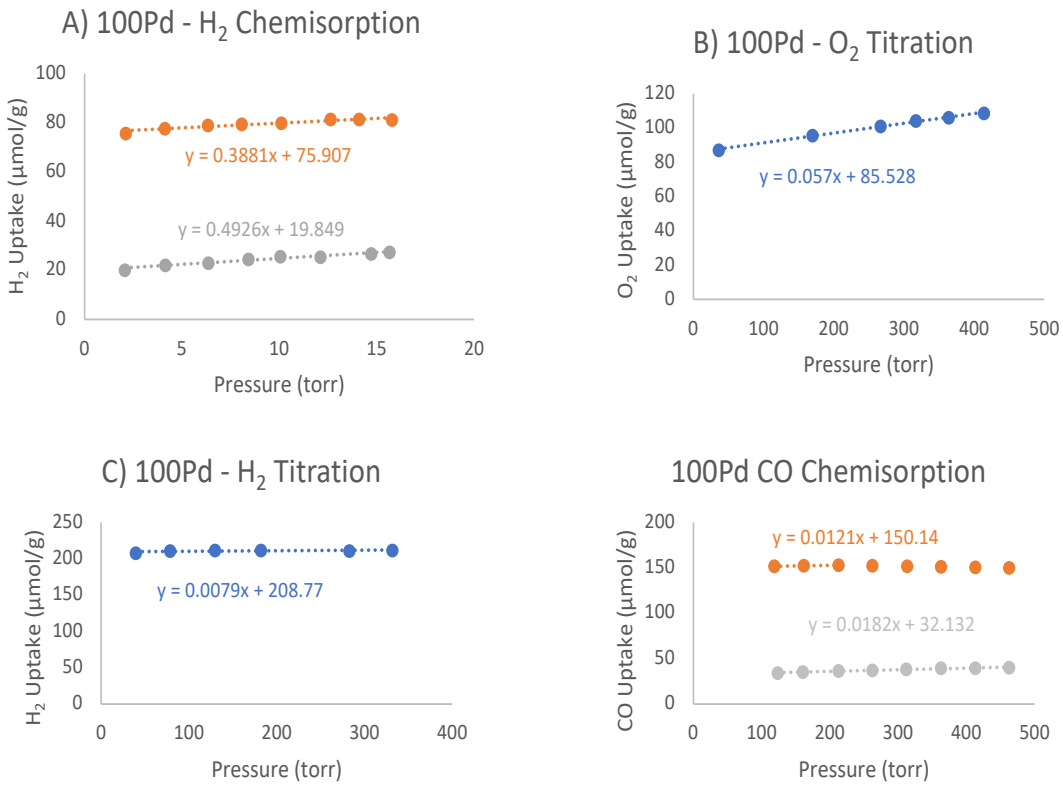

Figure 3.1: Representative measurements for A) H_2 chemisorption at 35 °C, B) subsequent O_2 titration of the preadsorbed hydrogen at 35 °C, C) H_2 titration of the preadsorbed oxygen at 100 °C, and D) CO chemisorption at 35 °C after evacuation at 100 °C. Orange lines are uptake on the palladium and silica support and grey is uptake on silica. CO uptake points are excluded from pressures of 210 torr to 500 torr to avoid a negative slope in the linear fit.

Table 3.1: Uptake (μmol/g) and uncertainties in y-intercepts using a linear fit for volumetric uptakes. 1st isotherm is uptake on palladium and support and 2nd isotherm is uptake on the support.

Catalyst	H_2 1st Isotherm	H_2 2nd Isotherm	H_2 uptake	O_2 titration	H_2 titration	CO 1st Isotherm	CO 2nd Isotherm	CO uptake
100Pd	76 ± 1	20 ± 0.4	56 ± 1	86 ± 1	209 ± 2	150 ± 1	32 ± 1	118 ±1

After the hydrogen chemisorption was completed, the surface was titrated with oxygen, as shown in Figure 3.1 B. The uptake of 86 μmol/g can be converted to a Pd site density using the stoichiometry factor of 4/3, according to equation 1.2, resulting in 115 μmol/g or a dispersion of 60%.

After the oxygen titration was completed, the surface was titrated with hydrogen, as shown in Figure 3.1 C. The uptake of 209 μmol/g can be converted to a Pd site density using the stoichiometry factor of 2/3, according to equation 1.1, resulting in 139 μmol/g or a dispersion of 73%.

The oxygen remaining on the surface was then desorbed by evacuating at 100 °C. Then an analysis of the site density by CO chemisorption was performed, as shown in Figure 3.1 D. The uptake of 118 μmol CO/g is equal to the Pd site density assuming a SF of 1, which results in a Pd dispersion of 61%.

To assess the reproducibility of the chemisorption and titration measurements, three trials using separate samples of the parent catalyst were performed and the results are shown in Table 3.2. The uncertainty in the hydrogen chemisorption for the parent catalyst of ±3 μmol/g was calculated at a 95% confidence interval for the three trials. For subsequent measurements, the reported amount of exposed palladium will be reported with an uncertainty of ±3 μmol/g. The

uncertainty for H_2 titration was 4 μmol/g for three trials. Therefore, 4 μmol/g will be used to report the amount of exposed palladium for titration measurements on other catalysts.

Table 3.2: Palladium site density (μmol/g) of catalyst for three different trials with reported averages and uncertainties at a 95% confidence interval.

	Trial 1	Trial 2	Trial 3	Average
H_2 Chemisorption	112 ±2	107 ±2	112 ±3	110±4
H_2 Titration	139 ±1	132 ±1	133 ±1	135±2

A summary of the dispersion and particle sizes using the two titration and two chemisorption techniques is given in Table 3.3, along with the stoichiometry factor (SF) values from Benson and Boudart.[22] The particle size, *d*, was calculated from the dispersion,

$$d = \frac{1.1}{D}, \tag{3.2}$$

where *D* is the dispersion and the particle size is in *nm*, following the standard convention.[32]

Table 3.3: Palladium dispersion, particle size, and assumed SF used in gas adsorption methods.

Technique	Dispersion (%)	Particle size (nm)	Stoichiometry Factor (mol Pd/mol adsorbate)
H_2 Chemisorption	60	1.8	2
O_2 Titration	61	1.8	4/3
H_2 Titration	74	1.5	2/3
CO Chemisorption	65	1.7	1

Evidence gathered here from all four gas adsorption techniques for the 2 wt% Pd/SiO_2 parent catalysts shows that the dispersion of the catalyst made by ion exchange is comparable to previous work using this method. The average dispersion from all 4 techniques is 65% with a standard deviation of 7%. Because the statistical uncertainty in the hydrogen chemisorption and titration measurements are small compared to the difference between the calculated Pd site density, the variation in quantified palladium dispersion is most likely due to the accuracy of the idealized stoichiometry factors.

What is interesting is how well these profiles compare to earlier work by Chou and Vannice.[29] For a 2.10 wt% Pd/SiO_2 catalyst (made in the same way as the catalysts in this thesis through ion-exchange using $Pd(NO_3)_2{\cdot}4NH_3$), the CO chemisorption uptake was quantified as 127.5 μmol/g at 300K. This is close to the value reported here of 121 μmol/g. The higher CO uptake of the 1987 study makes sense because there is slightly more palladium. The wt % of the catalyst used in Vannice's study was verified by plasma emission spectroscopy and neutron activation analysis. While the Pd wt % was not verified for the parent catalyst used in this thesis,

the comparison in how closely the CO chemisorption profiles match between the catalyst in this thesis and Vannice's work indicates that the catalysts created here with the ion exchange technique have a Pd loading expected based on the amount of Pd used in the synthesis. Also reported in the study by Chou and Vannice[29] was a hydrogen chemisorption uptake of 67 μmol/g and scaling this by the same palladium wt % ratio yields 64 μmol/g which is close to the average H_2 chemisorption uptake reported here of 56 +/- 3 μmol/g.

For comparison, in the 1973 Boudart study, the variation in reported dispersion for the same four gas adsorption techniques under the same conditions is about 7%.[22] Despite these systematic differences in the estimated dispersion, the characterization of the parent Pd/SiO_2 catalysts indicates that the pretreatment conditions employed was successful in preparing the parent catalyst and that the sequence of reduction, H_2 chemisorption, O_2 titration, H_2 titration, and CO chemisorption resulted in amounts of exposed palladium consistent with previous work.

Note that in Table 3.3, the stoichiometry factors are based on idealized models of how the adsorbates populate the Pd surface and oversimplify the quantification of the palladium site density. To illustrate this point, Alba-Rubio et al. show a transmission IR spectrum of CO adsorbed on highly dispersed 3.5 wt % Pd monometallic Pd/SiO_2 and 3.1 wt % Au bimetallic $Pd-Au/SiO_2$ catalysts.[30] The spectrum of the bimetallic catalyst in that study represents that there is significant reduction in linear binding when gold is added. Interestingly, for their low dispersion catalyst, the ratio of bent to linear IR bands did not have a significant change. For this catalyst in the study, the number of palladium sites in μmol/g decreased from 91 to 28 (assuming a 0.67 CO/Pd stoichiometry which isn't appropriate for Pd-Au catalysts because the distribution of CO bridge vs linear sites isn't the same as pure palladium) with the addition of gold making the bimetallic catalyst 1 wt % in Au. In the context of the evidence gathered for this study, one

would need to verify the CO stoichiometry with IR data for each catalyst and interpret how these measured stoichiometries correlate to quantifiable CO uptake and by extension, the number of exposed palladium sites.

Adding another level of complexity to the idea of knowing correct surface stoichiometries, the effect of surface segregation upon the adsorption of CO on the palladium sites can be considered. Kunz et al. showed that this can occur due to heating the surface from 273K to 323K according to their IR data.[12] They showed that for a 50Pd50Au Pd-Au/Al_2O_3 catalyst the band at 2105 cm^{-1} that corresponds to CO bound linearly to gold sites significantly decreases going from 273K to 323K. At the higher temperature, the IR bands that correspond to CO bound in a linear orientation to palladium decreased while the bent orientation increased. The ratio for the number of bridged sites over the number of linear sites at 273K is 0.99 and at 323K is 1.89. This would then suggest that at the CO chemisorption analysis temperature used here at 308K for the bimetallic catalyst there is a mixture of bent and linear CO adsorption geometries. Therefore, the stoichiometry factor assumed according to Boudart et al.[22] being 1Pd:1CO is most likely not accurate for the application of bimetallic catalysts used here.

3.2 Au/Pd preparation and characterization

The composition of the AuPd bimetallic catalysts was determined using ICP-OES and compared to the gold loading used in the synthesis. Table 3.4 shows the mass of the gold hydrate used in the synthesis to calculate the gold loading, assuming that the precursor was the monohydrate. The results of the ICP analysis were converted into gold loadings based on the mass of catalyst digested. As shown, the gold loading determined by ICP is larger by about a factor of two. The masses measured of the $HAuCl_4$ hydrate may not be entirely correct because the precursor is hygroscopic and takes in water very easily. This can overcount the true gold

mass and ICP should have determined a mass less than what was used in the synthesis. If the gold loading from the synthesis is compared to the exposed Pd site density of 112 μmol Pd/g catalyst, based on H_2 chemisorption, then the amount of gold can cover from about 1/3 to 90% of the Pd particle surfaces. However, if the ICP analysis is correct, then the gold loading for AuPd-2, -3, and -4 is more than enough to completely cover the Pd particles. If the ICP results are accurate, we would expect to measure exposed palladium in the chemisorption and titration techniques only for catalyst AuPd-1.

Table 3.4: Actual gold hydrate mass and corresponding loading used in synthesis of $AuPd/SiO_2$ catalysts, gold concentration in the digest from ICP, and quantified gold loadings based on ICP results.

Sample	Mass of Au hydrate used in synthesis of catalyst (g)	Gold loading based on synthesis (μmol Au/g catalyst)	Concentration of gold from ICP analysis (ppm)	Gold loading based on ICP analysis (μmol Au/g catalyst)
AuPd-1	0.00924	37	15.5	77
AuPd-2	0.0121	48	22.8	225
AuPd-3	0.0194	77	24.5	130
AuPd-4	0.02515	100	45.6	134

The composition of the AuPd bimetallic catalysts can be estimated from the ratio of the gold loadings to the Pd loading based on the synthesis, as described in Sect. 3.1, and shown in

Table 3.5. The ICP analysis results in a higher bulk Au composition than the estimates based on the Pd and Au used in the synthesis. These ratios provide an indication of the composition of the particles if a homogeneous alloy is formed.

Table 3.5: Ratio of mass loadings [(μmoles Au/g cat)/(μmoles Pd/g cat)] from the IWI synthesis procedure and the ICP analysis.

Sample	IWI synthesis procedure	ICP Analysis
AuPd-1	0.19	0.40
AuPd-2	0.25	1.17
AuPd-3	0.40	0.68
AuPd-4	0.52	0.70

3.3 Chemisorption measurements on Au-Pd/SiO_2 Catalysts

The dispersions and palladium site density of the AuPd catalysts were characterized using chemisorption methods. The isotherm chemisorption profiles on the catalysts shown in Figure 3.2 are consistent with what was described in section 3.1, where the isotherm with the greatest uptake corresponds to adsorption on the palladium plus the support and the isotherm with the smallest uptake is adsorption only on the support, because adsorbates are already bound to palladium sites, and the difference between the two is the amount of adsorbate bound on palladium. The differences between the two are expected to be smaller than in the parent catalyst because gold on the surface should block some palladium sites.

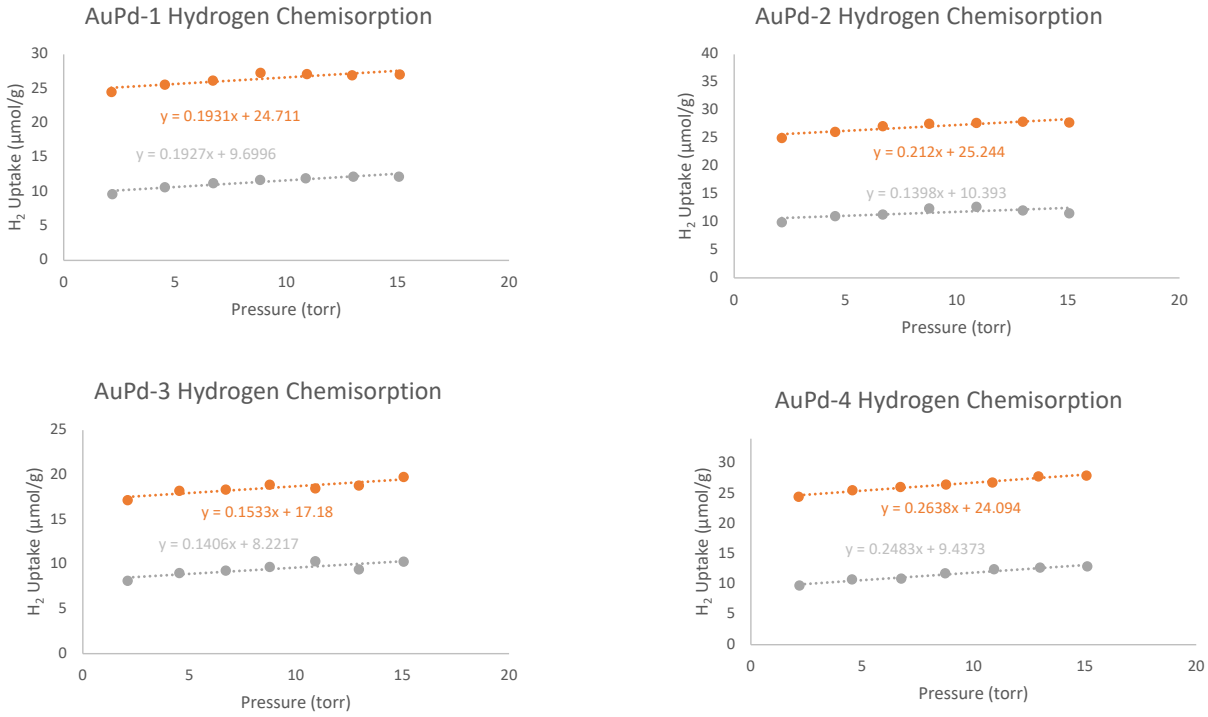

Figure 3.2: Representative hydrogen chemisorption measurements at 35 °C for each bimetallic palladium-gold catalyst samples. Orange lines are uptake on the palladium and silica support and grey is uptake on silica.

The difference between the uptake in the 1st and 2nd isotherms for hydrogen chemisorption for all bimetallic catalyst samples is shown in Table 3.6. For multiple measurements of the same catalyst, the results shown are average values. For sample AuPd-1, the difference is 14.5±1 μmol H_2/g. The palladium site density takes into account the stoichiometry of reaction 3.1 and therefore, the palladium site density is 29 ± 2 μmol/g. The dispersion can be calculated directly from the ratio to the Pd loading of 192 μmol/g to be 15%. For sample AuPd-2, the difference between the uptake in the 1st and 2nd isotherm is 16.3, the palladium site density is 32.6 ± 2 μmol/g, and the dispersion is 17%. For sample AuPd-3, the difference between the uptake in the 1st and 2nd isotherm is 11.3, the palladium site density is 22.6 ± 2 μmol/g, and the dispersion is 12%. For sample AuPd-4, the difference between the uptake in the 1st and 2nd isotherm is 14.6, the palladium site density is 29.2 ± 2 μmol/g, and the dispersion is 15%. Effectively, the amount of surface exposed palladium is relatively constant, even with an increase in gold loading between each sample.

Table 3.6: Uptake (μmol/g) and uncertainties in y-intercepts using a linear fit for volumetric uptakes on the bimetallic catalysts. 1st isotherm is uptake of palladium and support and 2nd isotherm is uptake of the support.

Catalyst	H_2 1st Isotherm	H_2 2nd Isotherm	H_2 uptake	O_2 titration	H_2 titration	CO 1st Isotherm	CO 2nd Isotherm	CO uptake
AuPd-1	24.5±0.4	10.0±0.3	14.5±0.5	30.0±0.2	70±1	37.6±0.9	11.2±0.3	26.4±0.9
AuPd-2	26.5±0.4	10.2±0.5	16.3±0.6	26.4±0.5	69±1	43.3±0.5	12.5±0.6	30.8±0.8
AuPd-3	18.8±0.3	7.5±0.2	11.3±0.4	25.7±0.7	65±1	30.1±0.8	9.3±0.4	20.8±0.9
AuPd-4	23.3±0.3	8.7±0.3	14.6±0.4	24.3±0.5	61±1	30±1	12±2	18±2

After the hydrogen chemisorption was completed, the surface was titrated with oxygen, as shown in Figure 3.3. For the AuPd-1 sample, the uptake shown in Table 3.6 is 30.0 ± 0.2 µmol/g. This can be converted to a Pd site density using the stoichiometry factor of 4/3, according to equation 1.2, resulting in 40 µmol/g or a dispersion of 21%. For the AuPd-2 sample, the uptake shown in Table 3.6 is 26.4 ± 0.5 µmol/g. This can be converted to a Pd site density using the stoichiometry factor of 4/3, according to equation 1.2, resulting in 35 µmol/g or a dispersion of 18%. For the AuPd-3 sample, the uptake shown in Table 3.6 is 25.7 ± 0.7 µmol/g. This can be converted to a Pd site density using the stoichiometry factor of 4/3, according to equation 1.2, resulting in 34 µmol/g or a dispersion of 18%. For the AuPd-1 sample, the uptake shown in Table 3.6 is 24.3 ± 0.5 µmol/g. This can be converted to a Pd site density using the stoichiometry factor of 4/3, according to equation 1.2, resulting in 32 µmol/g or a dispersion of 17%.

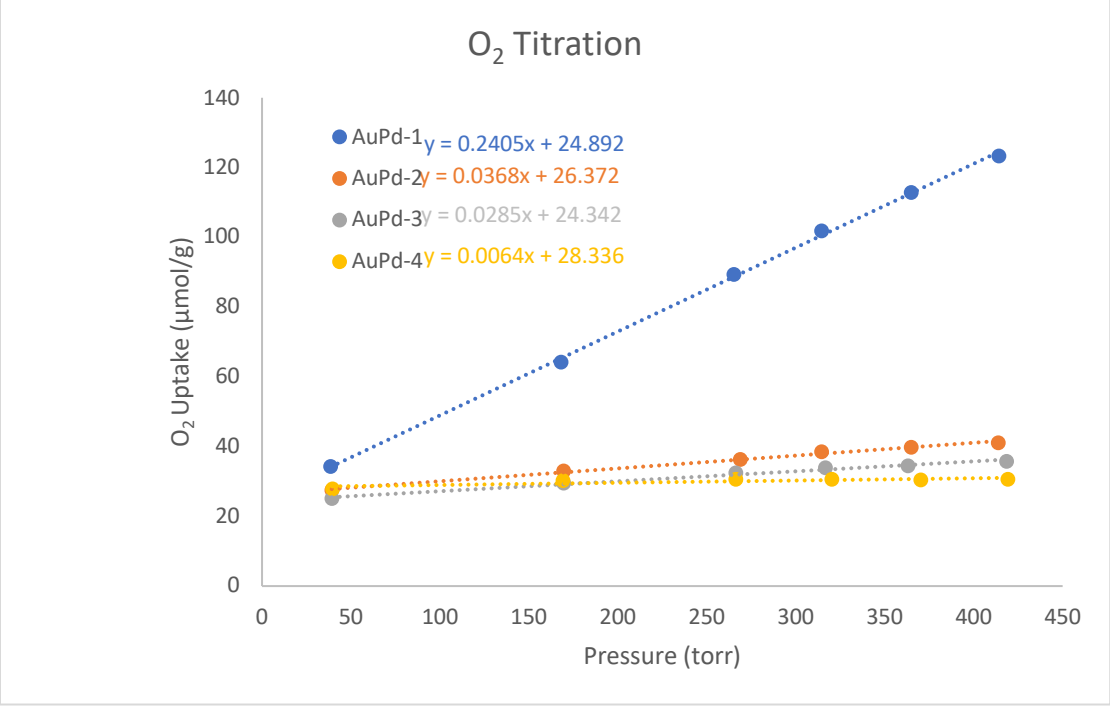

Figure 3.3: Oxygen titration results at 35 °C for samples AuPd-1 to AuPd-4 with linear fits.

After the oxygen titration was completed, the surface was titrated with hydrogen, as shown in Figure 3.4. For the AuPd-1 sample, the uptake shown in Table 3.6 is 70 ± 1 µmol/g. This can be converted to a Pd site density using the stoichiometry factor of 2/3, according to equation 1.1, resulting in 47 µmol/g or a dispersion of 24%. For the AuPd-2 sample, the uptake shown in Table 3.6 is 69 ± 1 µmol/g. This can be converted to a Pd site density using the stoichiometry factor of 2/3, according to equation 1.1, resulting in 46 µmol/g or a dispersion of 24%. For the AuPd-3 sample, the uptake shown in Table 3.6 is 64.9 ± 0.8 µmol/g. This can be converted to a Pd site density using the stoichiometry factor of 2/3, according to equation 1.1, resulting in 43 µmol/g or a dispersion of 22%. For the AuPd-1 sample, the uptake shown in Table 3.6 is 61± 1 µmol/g. This can be converted to a Pd site density using the stoichiometry factor of 2/3, according to equation 1.1, resulting in 41 µmol/g or a dispersion of 21%.

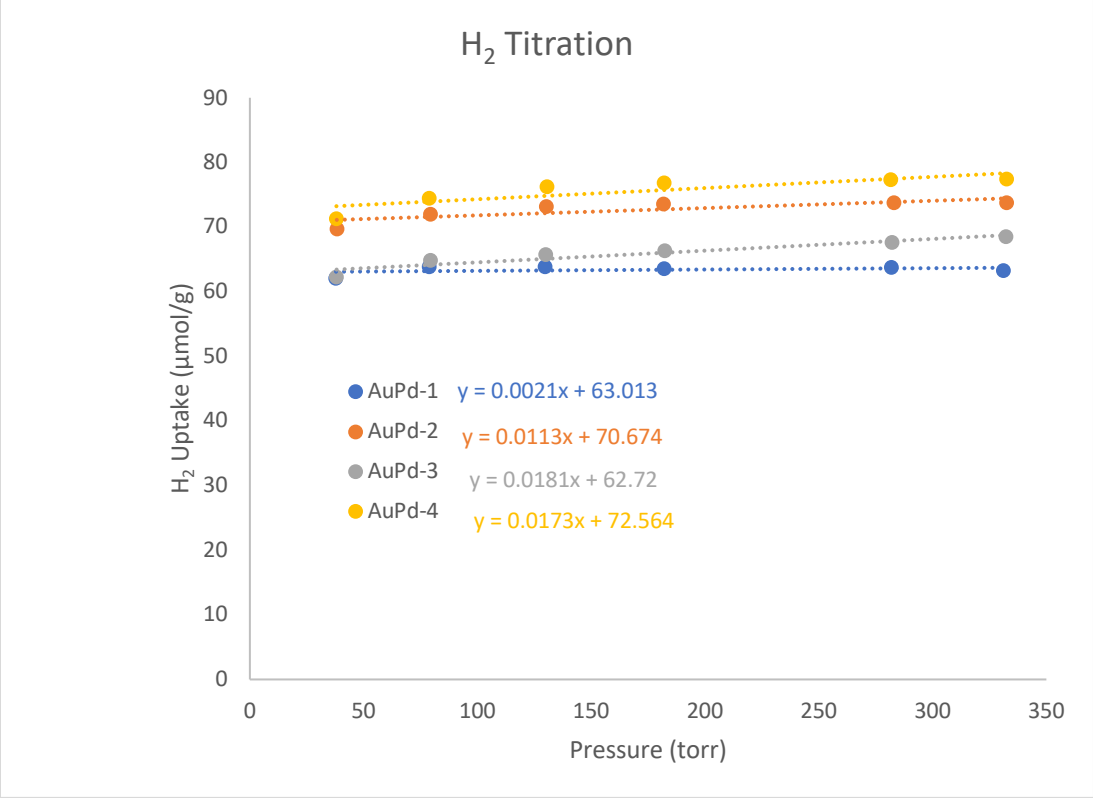

Figure 3.4: Hydrogen titration results at 100˚C for samples AuPd-1 to AuPd-4 with linear fits.

The oxygen remaining on the surface was then desorbed by evacuating at 100 °C. Then an analysis of the site density by CO chemisorption was performed, as shown in Figure 3.5. For the AuPd-1 sample, the measured uptake of 26.4 µmol CO/g shown in Table 3.6 is equal to the Pd site density assuming a SF of 1, which results in a Pd dispersion of 14%. For the AuPd-2 sample, the measured uptake of 30.8 µmol CO/g shown in Table 3.6 is equal to the Pd site density assuming a SF of 1, which results in a Pd dispersion of 16%. For the AuPd-3 sample, the measured uptake of 20.8 µmol CO/g shown in Table 3.6 is equal to the Pd site density assuming a SF of 1, which results in a Pd dispersion of 11%. Finally, for the AuPd-1 sample, the measured uptake of 18 µmol CO/g shown in Table 3.6 is equal to the Pd site density assuming a SF of 1, which results in a Pd dispersion of 9%.

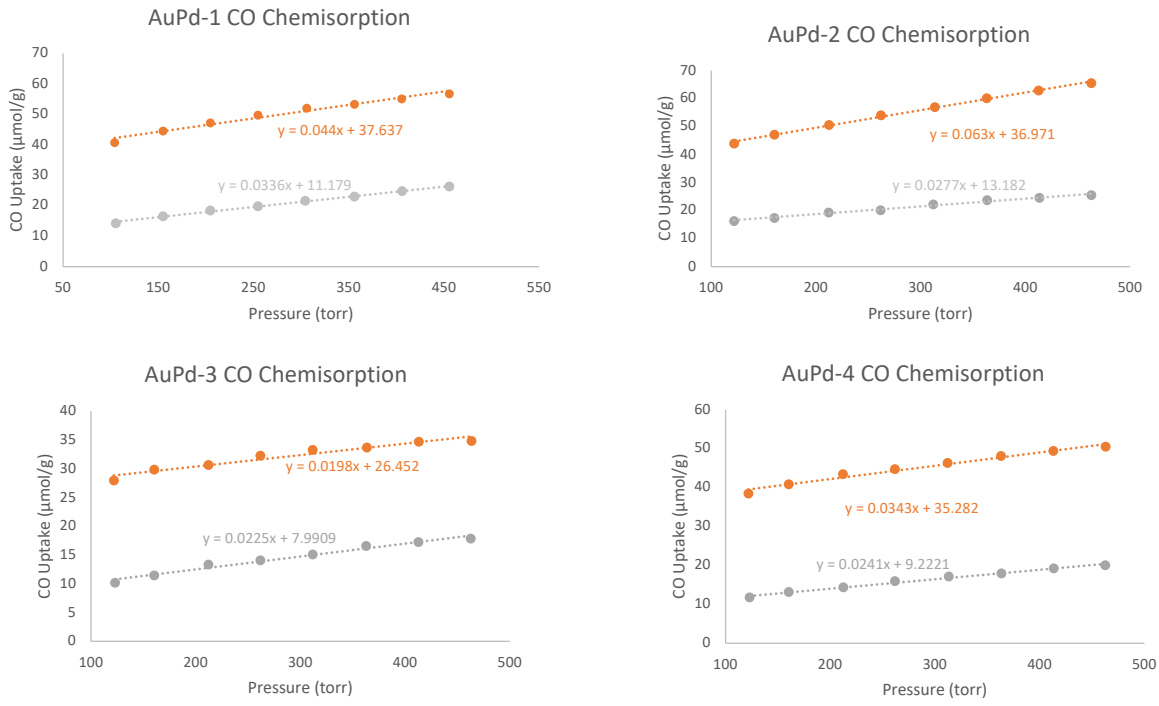

Figure 3.5: Representative carbon monoxide chemisorption measurements at 35 °C for each bimetallic palladium-gold catalyst sample. Orange lines are uptake on the palladium and silica support and grey is uptake on silica.

According to Vannice, titration offers an advantage over chemisorption techniques because of the increased sensitivity, and it can eliminate possible surface contamination.[18] However, it is possible that the oxygen predosed onto the nanoparticle can cause surface segregation of Pd. In the standard method used here, the palladium surface was saturated with oxygen and then titrated with hydrogen. For example in the AuPd-1 catalyst, the previously H_2 chemisorbed sample was titrated with O_2 measuring 40 +/-4 μmol/g of palladium and then the preabsorbed oxygen atoms were then titrated with H_2 measuring 48 +/-4 μmol/g. Alba-Rubio et al. have also shown that gold atoms in gold-palladium catalysts do not bind oxygen in their hydrogen peroxide decomposition reaction on their Pd-Au/SiO_2 catalysts.[30] One needs to also consider possible surface migration of hydrogen atoms to gold even though it is believed that hydrogen should dissociate at Pd sites only. If the migration were possible, the different stoichiometries in the two titration methods described in the introduction and seen below could show a significant difference in the number of palladium sites:

$$Pd_S H + \tfrac{3}{4} O_2 \rightarrow Pd_S O + \tfrac{1}{2} H_2 O \qquad \text{Oxygen titration} \quad (3.3)$$

$$Pd_S O + \tfrac{3}{2} H_2 \rightarrow Pd_S H + H_2 O \qquad \text{Hydrogen titration} \quad (3.4)$$

One would then expect the palladium site density in hydrogen titration to be lower than oxygen titration. The difference in site density is 8 +/-4 μmol/g between the two techniques, and so either surface segregation or hydrogen migration may be possible.

Both H_2 and O_2 titration results shown in Figures 3.3 and 3.4 indicate that as more gold is added, the y-intercept for the uptake extrapolated back at zero pressure decreases. There is a reduction to about 30% in uptake compared with the site density with the monometallic catalyst, as shown in Figure 3.6. However, if one considers the uncertainty of 4 μmol/g catalyst there is not a significance difference in Pd site density between the catalyst samples.

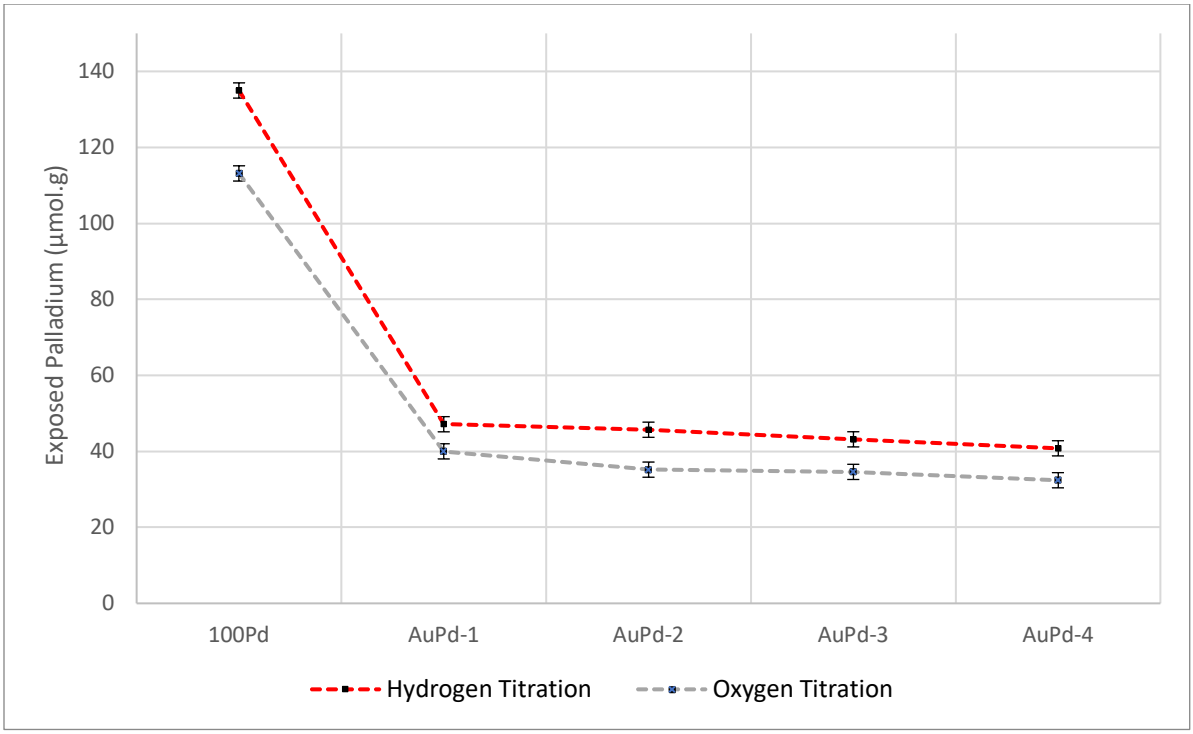

Figure 3.6: Averages of titration results plotted with increasing gold mol percent. Dotted line is added to guide the eye and show trend.

The exposed palladium measured with the chemisorption methods gives similar results to the titration measurements, as shown in Figure 3.7. For the three trials in hydrogen chemisorption for the AuPd-3 catalyst, the average palladium site density is 23 µmol/g, the standard deviation is 5 µmol/g, and the uncertainty at a 95% confidence interval is 6 µmol/g. Considering the average and this uncertainty of 23 +/- 6 µmol/g of exposed palladium, the chemisorption result ranges from 18 to 29 µmol/g. The average palladium site density of the AuPd-1 and AuPd-4 gold samples fall within this range and the average for the AuPd-2 sample is very close within this range. These results suggest that the same site density of palladium is being measured even with an increasing amount of gold between samples. If one applies this

logic to the CO chemisorption, the same conclusion can be made because all average amounts of exposed palladium within an uncertainty of +/- 6 µmol/g overlap with each other.

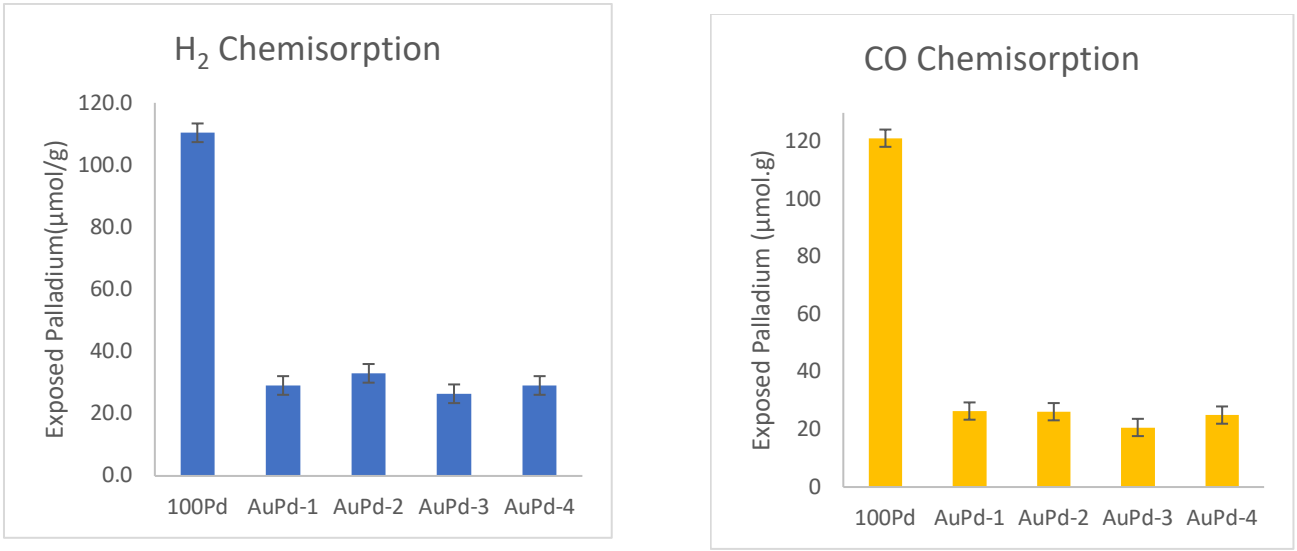

Figure 3.7: Averages of chemisorption results plotted for each catalyst sample. Error bars are based on the reproducibility for measurements on the Pd100 catalyst.

All of the uptake data for both chemisorption and titration is summarized in Table 3.7.

Table 3.7: Summary of exposed Pd site densities (μmol/g) for chemisorption and titration results for all techniques and all catalysts.

Sample	H_2 Chemisorption 1	H_2 Chemisorption 2	H_2 Chemisorption 3	H_2 Chemisorption Average
100Pd	112	107	112	110
AuPd-1	28	30	-	29
AuPd-2	30	36	-	33
AuPd-3	20	18	30	23
AuPd-4	29	29	-	29
Sample	**O_2 Titration 1**	**O_2 Titration 2**	**O_2 Titration 3**	**O_2 Titration Average**
100Pd	114	112	-	113
AuPd-1	40	-	-	40
AuPd-2	35	-	-	35
AuPd-3	33	35	-	34
AuPd-4	32	-	-	32
Sample	**H_2 Titration 1**	**H_2 Titration 2**	**H_2 Titration 3**	**H_2 Titration Average**
100Pd	133	133	139	135
AuPd-1	48	-	-	48
AuPd-2	46	-	-	46
AuPd-3	41	45	-	43
AuPd-4	41	-	-	41
Sample	**CO Chemisorption 1**	**CO Chemisorption 2**	**CO Chemisorption 3**	**CO Chemisorption Average**
100Pd	118	-	-	118
AuPd-1	26	-	-	26
AuPd-2	27	25	-	26
AuPd-3	18	23	-	21
AuPd-4	25	-	-	25

Additional experiments were performed on 3 of the 4 bimetallic catalysts of independent hydrogen titration runs where each sample was soaked in flowing oxygen at 100 °C for an hour before performing the titration and the results can be seen in Figure 3.8. Converting the uptakes

using a SF of 2/3 give exposed palladium site densities of 56.8 µmol/g for AuPd-2, 53.6 for AuPd-3, and 52 for AuPd-4. The effect compared to the results in Figure 3.6 is larger, where the number of exposed palladium sites is higher in all three catalysts compared to the hydrogen titration experiments that were done in the tandem method described earlier. This indicates that flowing in oxygen likely causes some surface segregation of the palladium.

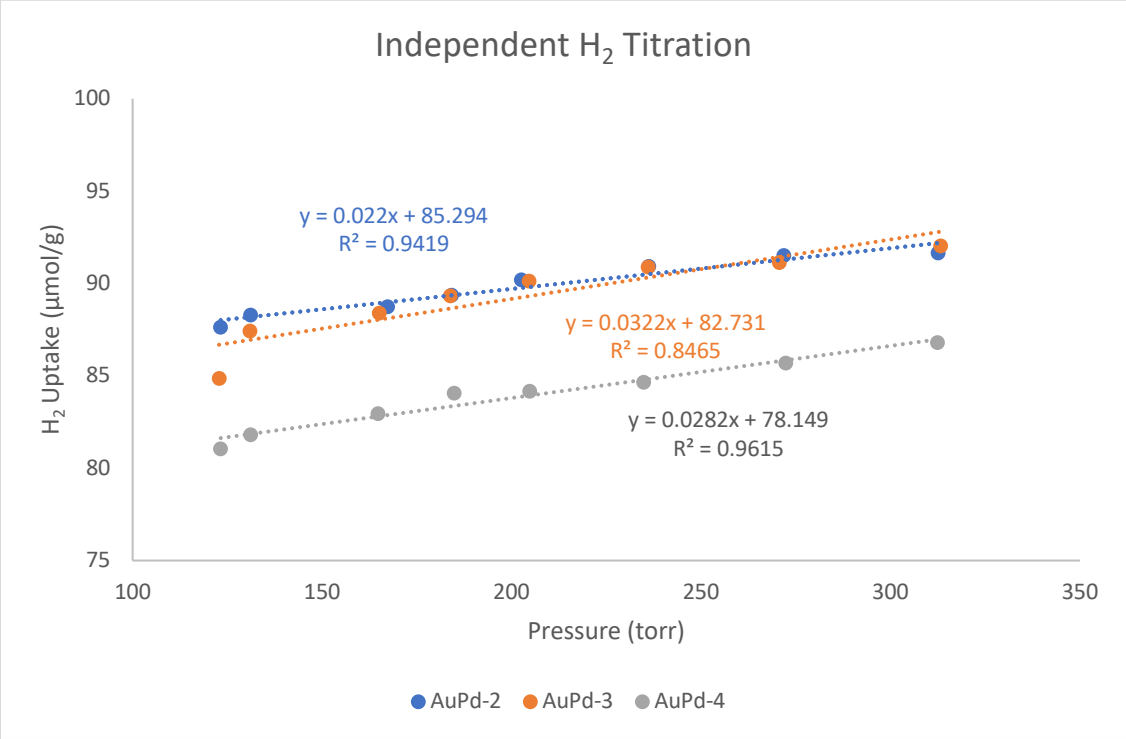

Figure 3.8: Results in uptake for a separate hydrogen titration set of experiments with quantified amount of exposed palladium.

3.4 Interpretation of chemisorption data

In work by Monnier et al, they synthesized Pd-Au/SiO_2 bimetallic catalyst samples with varying gold loadings using the technique of electroless deposition to deposit gold on a 1.86 wt% Pd/SiO_2 catalyst.[24] They characterized each catalyst sample with various techniques including hydrogen pulse titration of preadsorbed oxygen. During the pretreatment processes of preparing the catalysts for pulse titration, each sample was reduced at 200˚C during hydrogen reduction, exposed to 100% Ar for 1 hr at 200˚C to remove chemisorbed hydrogen, cooled to 40˚C, and exposed to 10% O_2/balance Ar to saturate the palladium surface with atomic oxygen. In Figure 7 of the study, there was a higher uptake in the 0.5 wt% Au catalyst (0.08 +/- 0.02 mL hydrogen STP/g catalyst) than the 2 wt% Au catalyst (0.02 +/- 0.01 mL hydrogen STP/g catalyst) and this evidence shows within their level of uncertainty for the measurements that there are less exposed palladium sites with the catalyst of a higher weight percent gold. Their parent catalyst is 1.86 wt % Pd and if their bimetallic catalyst with the highest gold loading is 2 wt% Au, then all of the gold should have deposited on the palladium. However, they still detected palladium sites even at the highest gold loading.

To have a site balance on each of the bimetallic catalysts, the fraction of Pd covered by gold plus the fraction of palladium not covered must equal 1. Since the chemisorption and titration techniques only measure the amount of palladium on the surface of the catalysts and that the site density of the 100Pd catalyst was measured for each technique, the fraction of the palladium on the surface covered by gold (θ_{Au}) on each catalyst is:

$$\theta_{Au} = 1 - \theta_{Pd} \tag{3.5}$$

$$\theta_{Au} = 1 - \frac{Measured\ Pd\ site\ density\ on\ Bimetallic\ catalyst}{Measured\ site\ density\ on\ 100Pd} \tag{3.6}$$

Applying this formulation on the experimental results for the average amount of exposed palladium seen in Table 3.7, the corresponding data for each technique is shown in Table 3.8:

Table 3.8: Apparent surface coverage of gold based on experimental data. Uncertainties are estimated to be ±0.01.

Catalyst	H2 Chemisorption	O2 titration	H2 titration	CO chemisorption
100Pd	0	0	0	0
AuPd-1	0.74	0.65	0.65	0.78
AuPd-2	0.70	0.69	0.66	0.78
AuPd-3	0.76	0.69	0.68	0.83
AuPd-4	0.74	0.71	0.70	0.79

The results in Table 3.8 indicate that the surface coverage of gold is roughly 70% for all the bimetallic catalysts and there is good agreement between the different chemisorption and titration methods. The coverage estimates from the chemisorption methods are slightly higher than the estimates in the titration methods. If you compare the gold loadings used in the IWI synthesis (Table 3.4) to the amount of exposed surface palladium on the 100Pd catalyst, the fraction of gold surface coverage ranges from 28% to 77%. This implies that the amount gold for catalysts AuPd-1,-2,-3 is not enough to achieve the fractional gold coverage of 70%. On the other hand, if you compare the gold loadings determined by ICP analysis (Table 3.4) to the amount of exposed surface palladium on the 100Pd catalyst, the fraction of gold surface

coverage could range from 60% to 170%. This implies that the amount of gold is enough to completely cover all the palladium particles on all bimetallic catalysts except for AuPd-1.

This means that for the other catalyst samples, the question is why there is still exposed palladium. One possibility is that not all the gold adsorbed on palladium particles and could have adsorbed on other places on the support such as in its own independent nanoparticle clusters. In this case gold could be forming pure gold nanoparticles on the surface in addition to covering about 70% of palladium nanoparticles. A second possibility is that during some of the pretreatment steps some of the gold goes into the interior of the nanoparticles and palladium can segregate to the surface.

3.5 Conclusions and Future work

In this thesis we have synthesized a 2 wt% Pd/SiO_2 parent catalyst and characterized surface properties with chemisorption and titration methods. The measured dispersion ranged from 60-72% which is consistent with previous measurements for catalysts synthesized with the same loading and synthesis technique. A set of four bimetallic catalysts with varying gold loading were synthesized by incipient wetness impregnation. Each catalyst was digested in aqua-regia and the total gold content was determined by ICP-OES. The gold loading determined from the ICP analysis was roughly twice the gold loading used in the IWI synthesis. Then each bimetallic catalyst was characterized using chemisorption and titration methods and the fractional gold coverage was found to be about 70% independent of the gold loading. Based on the gold loadings from the IWI synthesis, a coverage of 70% gold could not have been possible except for the catalyst with the highest gold loading. Based on the gold loadings from ICP

analysis, there should have been enough gold to completely cover all palladium particles except for the catalyst with the lowest loading of gold.

Carrying this thesis work forward, more information about Pd/Au alloys and possible Au-Au clusters needs to be gathered. XRD would not be an effective way to achieve this because the determined particle size of ~2 nm is below the limit of detection. A more appropriate technique to determine the average chemical composition is XPS; however, it cannot provide spatial distribution of two metals on a support at the nanoscale level.[33] One could combine XPS information with EDS (energy dispersive X-ray spectroscopy) where, for example, raw EDS mapping data is grouped into a statistical two-dimensional data set that is able to tell how homogenous the composition is with two metals.

Chemisorption and titration data give information about the quantity of exposed Pd at the surface assuming a stoichiometry-based adsorption on one metal type. When a probe molecule interacts with bimetallic sites and bimetallic nanoclusters, the adsorption configuration of the probe could be different than the classic metal nanoparticles. For example, CO may be adsorbed on small metal clusters via the bridged configuration instead of the linear configuration. For this reason, IR spectra can be collected at different probe molecule coverages at various temperatures and reduction conditions to evaluate the reconstruction influence on bimetallic surfaces.

What can also be done for future work is to synthesize bimetallic catalyst using the technique of electroless deposition and see the effect of what changing reduction conditions has. During wetness impregnation, the gold is reduced on the surface in flowing hydrogen and there is a possibility that some of the gold deposited on the silica support in addition to the palladium atoms. In this case, one needs to consider if it's a more favorable process for the gold to form

nanoparticles on the silica support because of metal-metal interactions between gold particles than it would be for the gold to interact with the palladium. If electroless deposition is used, the palladium already on the surface acts as a catalyst for the reducing agent during the reduction process to only deposit the gold on the palladium and not the support.

BIBLIOGRAPHY

1. Martin, N. M.; Nilsson, J.; Skoglundh, M.; Adams, E. C.; Wang, X.; Smedler, G.; Raj, A.; Thompsett, D.; Agostini, G.; Carlson, S.; Norén, K.Study of Methane Oxidation over Alumina Supported Pd–Pt Catalysts Using Operando DRIFTS/MS and in Situ XAS Techniques. Catalysis, Structure and Reactivity, **2017**, 3, 24– 32

2. Persson K, Eriksson A, Jansson K, et al. Influence of molar ratio on Pd-Pt catalysts for methane combustion. J Catal**. 2006**, 243, 14–24.

3. V. Ponec, W.M.H. Sachtler; The reactions between cyclopentane and deuterium on nickel and nickel-copper alloys, Journal of Catalysis, **1972**, *24*, 250-261.

4. R. Davis, M. Boudart; Structure of Supported PdAu Clusters Determined by X-ray Absorption Spectroscopy, The Journal of Physical Chemistry**, 1994,** *98*, 5471-5477.

5. J.H. Sinfelt,; Supported "Bimetallic Cluster" Catalysts, Journal of Catalysis, **1973**, *29*, 308-315.

6. D. M. Alonso, S. G. Wettstein, J. A. Dumesic; Bimetallic catalysts for upgrading of biomass to fuels and chemicals, Chem. Soc. Rev., **2012**, *41*, 8075–8098.

7. G. W. Huber, J. W. Shabaker, S. T. Evans, J. A. Dumesic; Aqueous-phase reforming of ethylene glycol over supported Pt and Pd bimetallic catalysts, Applied Catalysis B: Environmental, **2006**, *62*, 226–235.

8. J. H. Sinfelt, Heterogenous Catalysis: Some Recent Developments, Science AAAS, **1977**, *195*, 641-646.

9. Y. L. Lam, M. Boudart; Preparation of Small Au-Pd Particles on Silica, Journal of Catalysis, **1977**, *50*, 530-540.

10. J. B. Darby; The Relative Heats of Formation of Solid Gold-Palladium Alloys, Acta Metallurgica, **1966**, *14*, 265-270.

11. Modelska, M., Binczarski, M.J., Kaminski, Z., Karski, S.; Kolesinska, B., Mierczynski, P., Severino, C.J., Stanishevsky, A., Witonska, I.A.; Bimetallic Pd-Au/SiO_2 Catalysts for Reduction of Furfural in Water. Catalysts, **2020**, *10*, 444-467.

12. S. Kunz, E. Iglesia; Mechanistic Evidence for Sequential Displacement−Reduction Routes in the Synthesis of Pd−Au Clusters with Uniform Size and Clean Surfaces, The Journal of Physical Chemistry**, 2014**, *118*, 7468-7479.

13. M. Mavrikakis, B. Hammer, J. K. Norskov; Effect of Strain Reactivity of Metal Surfaces, Physical Review Letters, **1998**, *81*, 2819-2822.

14. D.A. Dowden; Heterogenous Catalysis. Part I. Theoretical Basis, J. Chem. Soc., **1950,** *56*, 242.

15. K. W. Jacobsen, J. K. Norskov; Theory of Adsorbate-Induced Surface Relaxations: Hydrogen on Cu(110), Physical Review Letters, **1987**, *59*, 2764-2768.

16. A. Ruban, B. Hammer, P. Stoltze, H. L., J. K. Norskov; Surface electronic structure and reactivity of transition and noble metals, Journal of Molecular Catalysis A: Chemical, **1997**, *115*, 421-429.

17. M. Bonarowska, J. Pielaszek, W. Juszczyk, Z. Karpiński; Characterization of Pd–Au/SiO2 Catalysts by X-ray Diffraction, Temperature-Programmed Hydride Decomposition, and Catalytic Probes, Journal of Catalysis, **2000**, *195*, 304-315.

18. Albert M. Vannice, Kinetics of catalystic reactions, ONLINE, QD505. Volume 395 February **2005**, UMS Electronic Resources.

19. N. Krishnankutty and M. A. Vannice, J. Catal., **1995**, *155*, 312.

20. J. E. Benson, M. Boudart; Hydrogen-Oxygen Titration Method for the Measurement of Supported Platinum Surface Areas, Journal of Catalysis, **1965**, *4*, 704-710.

21. Armin Siebel, Yelena Gorlin, Julien Durst, Olivier Proux, Frédéric Hasché, Moniek Tromp, and Hubert A. Gasteiger; Identification of Catalyst Structure during the Hydrogen Oxidation Reaction in an Operating PEM Fuel Cell, ACS Catalysis**, 2016**, *11*, 7326-7334.

22. J. E. Benson, H. S. Hwang, M. Boudart; Hydrogen-Oxygen Titration Method for the Measurement of Supported Palladium Surface Areas, Journal of Catalysis, **1973**, *30*, 146-153.

23. K. D. Beard, J. W. Van Zee, J. R. Monnier; Preparation of carbon-supported Pt–Pd electrocatalysts with improved physical properties using electroless deposition methods, Applied Catalysis B: Environmental, **2009**, *88*, 185-193.

24. Rebelli, J., Detwiler, M., Ma, S., Williams, C. T., and Monnier, J. R.; Synthesis and characterization of Au-Pd/SiO2 bimetallic catalysts prepared by electroless deposition,. J. Catal., **2010**, *270*, 224-233.

25. B. Pawelec, A.M. Venezia, V. La Parola, E. Cano-Serrano, J.M. Campos-Martin, J.L.G. Fierro; AuPd alloy formation in Au-Pd/Al2O3 catalysts and its role on aromatics hydrogenation, Applied Surface Science, **2005**, *242*, 380-391.

26. J.H. Sinfelt, Chemical Engineering News, **July 1972,** 18.

27. M. Gsell, P. Jakob, and D. Menzel, Science, **1998**, 280, 717.

28. T. J. Schwartz, T. S. Wesley, J. A. Dumesic; Modifying the Surface Properties of Heterogeneous Catalysts Using Polymer-Derived Microenvironments, Top Catal, **2016**, 59, 19-2

29. P. Chou and M. A. Vannice, J. Catal. **1987**, 104, 17.

30. A. C. Alba-Rubio, A. Plauck, E. E. Stangland, M. Mavrikakis, J. A. Dumesic; Direct Synthesis of Hydrogen Peroxide Over Au–Pd Catalysts Prepared by Electroless Deposition, 2015, 145, 2057-2065.

31. Bergeret, G.; Gallezot, P., Particle Size and Dispersion Measurements. In *Handbook of Heterogeneous Catalysis*, pp 738-765.

32. T. Fovanna, M. Nachtegaal, A. H. Clark, O. Kröcher, D. Ferri; Preparation, Quantification, and Reaction of Pd Hydrides on Pd/Al_2O_3 in Liquid Environment*,* ACS Catalysis, **2023** *13* (5), 3323-3332.

33. L. Liu and A. Corma; Bimetallic Sites for Catalysis: From Binuclear Metal Sites to Bimetallic Nanoclusters and Nanoparticles, Chemical Reviews, **2023,** 123 (8), 4855-493.

34. J. Greeley, M. Mavrikakis; Alloy Catalysts Designed from First Principle, Nature Publishing Group, **2004**, 3, 810.

BIOGRAPHY OF THE AUTHOR

Andrew Thurstan Boucher was born on December 30, 1994 to John Carl and Diane Boucher. At two and a half years old he was adopted by Roger and Judy Boucher and grew up in their care in Byron, Maine with his twin brother Anthony Boucher. Growing up, he loved the outdoors in Maine and participated in many sports including tennis, soccer, and XC skiing. At 19 years of age, Andrew started at Saint Michael's College in Colchester, VT. He successfully received a B.S. in Chemistry in 2018 and then worked at Sappi in a research and development center in paper chemistry from 2018-2019. Knowing he wanted to further pursue academic studies, Andrew was accepted in the chemistry graduate program at The University of Maine Orono in 2019. He fell madly in love and soon became engaged to his lifelong partner Nancy Khattar on December 14, 2023. Andrew is excited to start a job in PFAFS chemistry as an organic environmental chemist through the DHHS at the state of Maine in Augusta. He is a candidate for the Master of Science degree in Chemistry from The University of Maine in December 2023.

Andrew and Nancy December 14, 2023